

Charged particle assisted nuclear reactions in solid state environment: renaissance of low energy nuclear physics

Péter Kálmán* and Tamás Keszthelyi†

*Budapest University of Technology and Economics,
Institute of Physics, Budafoki út 8. F., H-1521 Budapest, Hungary*

The features of electron assisted neutron exchange processes in crystalline solids are surveyed. It is found that, contrary to expectations, the cross section of these processes may reach an observable magnitude even in the very low energy case because of the extremely huge increment caused by the Coulomb factor of the electron assisted processes and by the effect of the crystal-lattice. The features of electron assisted heavy charged particle exchange processes, electron assisted nuclear capture processes and heavy charged particle assisted nuclear processes are also overviewed. Experimental observations, which may be related to our theoretical findings, are dealt with. The anomalous screening phenomenon is related to electron assisted neutron and proton exchange processes in crystalline solids. A possible explanation of observations by Fleischmann and Pons is presented. The possibility of the phenomenon of nuclear transmutation is qualitatively explained with the aid of usual and charged particle assisted reactions. The electron assisted neutron exchange processes in pure Ni , Pd and $Li - Ni$ composite systems (in the Rossi-type E-Cat) are analyzed and it is concluded that the electron assisted neutron exchange reactions in pure Ni and $Li - Ni$ composite systems may be responsible for recent experimental observations.

PACS numbers: 24.90.+d, 25.30.Fj, 25.40.Hs

Keywords: other topics in nuclear reactions: general, inelastic electron scattering to continuum, transfer reactions

I. INTRODUCTION

Since the "cold fusion" publication by Fleischmann and Pons in 1989 [1] a new field of experimental physics has emerged. Although even the possibility of the phenomenon of nuclear fusion at low energies is in doubt in mainstream physics, the quest for low-energy nuclear reactions (LENR) flourished and hundreds of publications (mostly experimental) have been devoted to various aspects of the problem. (For the summary of experimental observations, the theoretical efforts, and background events see e.g. [2], [3].) The main reasons for revulsion against the topic according to standard nuclear physics have been: (a) due to the Coulomb repulsion no nuclear reaction should take place at energies corresponding to room temperature, (b) the observed extra heat attributed to nuclear reactions is not accompanied by the nuclear end products expected from hot fusion experiences, (c) traces of nuclear transmutations were also observed, that considering the repulsive Coulomb interaction is an even more inexplicable fact at these energies.

Also in the last two decades, investigating astrophysical factors of nuclear reactions of low atomic numbers, which have great importance in nuclear astrophysics [4], [5], in the cross section measurements of the dd reactions in deuterated metal targets extraordinary observations were made in low energy accelerator physics [6], [7], [8], [9], [10], [11], [12]. The phenomenon of increasing cross

sections of the reactions measured in solids compared to the cross sections obtained in gaseous targets is the so called anomalous screening effect. Several years ago a systematical survey of the experimental methods applied in investigating and the theoretical efforts for the explanation of the anomalous screening effect was made [13] from which one can conclude that the full theoretical explanation of the effect is still open.

Motivated by the observations in the above two fields we search for physical phenomena that may have modifying effect on nuclear reactions in solid state environment. Earlier we theoretically found [14], [15] that if the reaction $p + d \rightarrow {}^3He$ takes place in solid material then the nuclear energy is mostly taken away by an electron of the environment instead of the emission of a γ photon, a result that calls the attention to the possible role of electrons. Concerning the assistance of the electrons and other charged constituents of the solid, a family of electron assisted nuclear reactions, especially the electron assisted neutron exchange process, furthermore the electron assisted nuclear capture process and the heavy charged particle assisted nuclear processes were discussed mostly in crystalline solid state (particularly in metal) environment [16], [17], [18]. The aim of this paper is to summarize our theoretical findings and on this basis to explain some experimental observations.

We adopt the approach standard in nuclear physics when describing the cross section of nuclear reactions. Accordingly, heavy, charged particles j and k of like positive charge of charge numbers z_j and z_k need considerable amount of relative kinetic energy E determined by the height of the Coulomb barrier in order to let the probability of their nuclear interaction have significant

*retired, e-mail: kalmanpeter3@gmail.com

†retired, e-mail: khelyi@phy.bme.hu

value. The cross section of such a process can be derived applying the Coulomb solution $\varphi(\mathbf{r})$,

$$\varphi(\mathbf{r}) = e^{i\mathbf{k}\cdot\mathbf{r}} f(\mathbf{k}, \mathbf{r}) / \sqrt{V}, \quad (1)$$

which is the wave function of a free particle of charge number z_j in a repulsive Coulomb field of charge number z_k [19], in the description of relative motion of projectile and target. In (1) V denotes the volume of normalization, \mathbf{r} is the relative coordinate of the two particles, \mathbf{k} is the wave number vector in their relative motion and

$$f(\mathbf{k}, \mathbf{r}) = e^{-\pi\eta_{jk}/2} \Gamma(1 + i\eta_{jk}) {}_1F_1(-i\eta_{jk}, 1; i[kr - \mathbf{k}\cdot\mathbf{r}]), \quad (2)$$

where ${}_1F_1$ is the confluent hypergeometric function and Γ is the Gamma function. Since $\varphi(\mathbf{r}) \sim e^{-\pi\eta_{jk}/2} \Gamma(1 + i\eta_{jk})$, the cross section of the process is proportional to

$$\left| e^{-\pi\eta_{jk}/2} \Gamma(1 + i\eta_{jk}) \right|^2 = \frac{2\pi\eta_{jk}(E)}{\exp[2\pi\eta_{jk}(E)] - 1} = F_{jk}(E), \quad (3)$$

the so-called Coulomb factor. Here

$$\eta_{jk}(E) = z_j z_k \alpha_f \sqrt{a_{jk} \frac{m_0 c^2}{2E}} \quad (4)$$

is the Sommerfeld parameter in the case of colliding particles of mass numbers A_j , A_k and rest masses $m_j = A_j m_0$, $m_k = A_k m_0$. $m_0 c^2 = 931.494 \text{ MeV}$ is the atomic energy unit, α_f is the fine structure constant and E is taken in the center of mass (CM) coordinate system.

$$a_{jk} = \frac{A_j A_k}{A_j + A_k} \quad (5)$$

is the reduced mass number of particles j and k of mass numbers A_j and A_k . Thus the rate of the nuclear reaction of heavy, charged particles of like positive charge becomes very small at low energies as a consequence of $F_{jk}(E)$ being very small.

In the processes investigated the Coulomb and the strong interactions play crucial role. The interaction Hamiltonian H_I comprises the Coulomb interaction potential V_{Cb} with the charged constituents of surroundings (solid) and the interaction potential V_{St} of the strong interaction:

$$H_I = V_{Cb} + V_{St}. \quad (6)$$

(The Coulomb interaction between the charged participants of the nuclear reaction is taken into account using (1).) Therefore the charged particle assisted nuclear reactions are at least second order in terms of standard perturbation calculation. According to (6), the lowest order of S-matrix element of a charged particle assisted nuclear reaction has two terms which can be visualized with the aid of two graphs. However, the contribution by the term, in which V_{St} according to chronological order precedes V_{Cb} , is negligible because of the smallness of the Coulomb factor the root square of which is appearing in

the matrix element of V_{St} in this case. (In the following we only depicts the graph of the dominant term.)

When describing the effect of the Coulomb interaction between the nucleus of charge number Z and a slow electron one can also use Coulomb function, consequently, the cross section of the process to be investigated is proportional to

$$F_e(E) = \frac{2\pi\eta_e(E)}{\exp[2\pi\eta_e(E)] - 1}, \quad (7)$$

but with

$$\eta_e = -Z\alpha_f \sqrt{\frac{m_e c^2}{2E}}. \quad (8)$$

Here m_e is the rest mass of the electron. In the case of low (less than 1 keV) kinetic energy of the electron $F_e(E)$ reads approximately as $F_e(E) = |2\pi\eta_e(E)| > 1$.

For instance, the cross section of electron assisted neutron exchange process (as it will be discussed later, and the graph of which is depicted in Fig. 1) is proportional to $F_e(E)$ only (instead of $F_{jk}(E)$) since the neutron takes part in strong interaction and so the corresponding matrix element does not contain Coulomb factor. The increment in the cross section due to changing $F_{jk}(E)$ for $F_e(E)$ in the case of electron assisted neutron exchange process can be characterized by the ratio $F_e(E)/F_{jk}(E)$ which is an extremely large number. The cross section of electron assisted neutron exchange process has a further (about a factor 10^{22}) increase due to the presence of the lattice since the cross section is also proportional to $1/v_c$. Here $v_c \sim d^3$ is the volume of the elementary cell of the solid with d the lattice parameter of order of magnitude of 10^{-8} cm . The extremely huge increment in the Coulomb factor increased further by the effect of the lattice makes it possible that the cross section of electron assisted neutron exchange process may reach an observable magnitude even in the very low energy case. Thus it can be concluded that the actual Coulomb factors are the clue to the charged particles assisted nuclear reactions and therefore we focus our attention to them especially concerning the Coulomb factors of heavy charged particles.

It is worth mentioning, that usual nuclear experiments, in which nuclear reactions of heavy charged particles are investigated, are usually devised taking into account the hindering effect of Coulomb repulsion. Consequently, the beam energy is taken to be appropriately high to reach the energy domain where the cross section of the processes becomes appropriately large. Therefore in an ordinary nuclear experiment the role of charged particle assisted reactions is not essential.

II. APPLIED METHOD PRESENTED IN ELECTRON ASSISTED NEUTRON EXCHANGE PROCESS

Recognizing the possibility and advantage of the assistance of electrons in LENR we consider first the electron

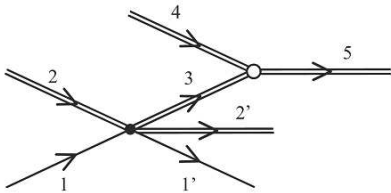
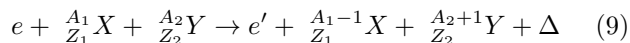


FIG. 1: The graph of electron assisted neutron exchange process. Particle 1 (and 1') is an electron, particle 2 is a nucleus which loses a neutron and becomes particle 2'. Particle 3 is an intermediate neutron. Particle 4 is the nucleus which absorbs the neutron and becomes particle 5. The filled dot denotes Coulomb-interaction and the open circle denotes nuclear (strong) interaction.

assisted neutron exchange process, namely the

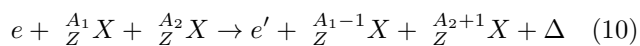


reaction [16] (see Fig.1). Here e and e' denote electron and Δ is the energy of the reaction, i.e. the difference between the rest energies of initial $\left(\frac{A_1}{Z_1}X + \frac{A_2}{Z_2}Y\right)$ and final $\left(\frac{A_1-1}{Z_1}X + \frac{A_2+1}{Z_2}Y\right)$ states.

In (9) the electron (particle 1) Coulomb interacts with the nucleus $\frac{A_1}{Z_1}X$ (particle 2). A scattered electron (particle 1'), the intermediate neutron (particle 3) and the nucleus $\frac{A_1-1}{Z_1}X$ (particle 2') are created due to this interaction. The intermediate neutron (particle 3) is captured due to the strong interaction by the nucleus $\frac{A_2}{Z_2}Y$ (particle 4) forming the nucleus $\frac{A_2+1}{Z_2}Y$ (particle 5) in this manner. All told, in (9) the nucleus $\frac{A_1}{Z_1}X$ (particle 2) loses a neutron which is taken up by the nucleus $\frac{A_2}{Z_2}Y$ (particle 4). The process is energetically forbidden if $\Delta < 0$. It was found, as it will be seen later, that the electron takes away negligible energy. In this process the Coulomb factor of electrons arises only since the particle, which is exchanged, is a neutron.

The physical background to the virtual neutron stripping due to the Coulomb interaction is worth mentioning. The attractive Coulomb interaction acts between the Z_1 protons and the electron. The neutrons do not feel Coulomb interaction. So one can say that in fact the nucleus $\frac{A_1-1}{Z_1}X$ is stripped of the neutron due to the Coulomb attraction.

As an example we take Ni and Pd as target material. It is thought that the metal (Ni or Pd) is irradiated with slow, free electrons. In this case reaction (9) reads as



with $Z = Z_1 = Z_2$.

Now we demonstrate our calculation. Let us take a solid (in our case a metal) which is irradiated by a monoenergetic beam of slow, free electrons. The corresponding sub-system Hamiltonians are H_{solid} and H_e . It is

supposed that their eigenvalue problems are solved, and the complete set of the eigenvectors of the two independent systems are known. The interaction between them is the Coulomb interaction of potential $V^{Cb}(\mathbf{x})$ and the other interaction that is taken into account between the nucleons of the solid is the strong interaction potential $V^{St}(\mathbf{x})$. In the second order process investigated an electron takes part in a Coulomb scattering with an atomic nucleus of the solid. In the intermediate state a virtual free neutron n is created which is captured due to the strong interaction with some other nucleus of the solid. The reaction energy Δ is shared between the quasi-free final electron and the two final nuclei which take part in the process. Since the aim of this paper is to show the fundamentals of the main effect, the simplest description is chosen.

The electron of charge $-e$ and the nucleus $\frac{A_1}{Z}X$ of charge Ze take part in Coulomb-interaction. We use a screened Coulomb potential of the form

$$V^{Cb}(\mathbf{x}) = \int \frac{-4\pi e^2 Z}{q^2 + \lambda^2} \exp(i\mathbf{q} \cdot \mathbf{x}) d\mathbf{q} \quad (11)$$

with screening parameter λ and coupling strength $e^2 = \alpha_f \hbar c$. For the strong interaction the interaction potential

$$V^{St}(\mathbf{x}) = -f \frac{\exp(-s|\mathbf{x}|)}{|\mathbf{x}|} \quad (12)$$

is applied, where the strong coupling strength $f = 0.08\hbar c$ [20] and $1/s$ is the range of the strong interaction. (\hbar is the reduced Planck constant, c is the velocity of light and e is the elementary charge.)

According to the standard perturbation theory of quantum mechanics the transition probability per unit time (W_{fi}) of this second order process can be written as

$$W_{fi} = \frac{2\pi}{\hbar} \sum_f |T_{fi}|^2 \delta(E_f - E_i - \Delta) \quad (13)$$

with

$$T_{fi} = \sum_{\mu} \frac{V_{f\mu}^{St} V_{\mu i}^{Cb}}{\Delta E_{\mu i}}. \quad (14)$$

Here $V_{\mu i}^{Cb}$ is the matrix element of the Coulomb potential between the initial and intermediate states and $V_{f\mu}^{St}$ is the matrix element of the potential of the strong interaction between the intermediate and final states, furthermore

$$\Delta E_{\mu i} = E_{\mu} - E_i - \Delta_{i\mu}. \quad (15)$$

E_i , E_{μ} and E_f are the kinetic energies in the initial, intermediate and final states, respectively, Δ is the reaction energy, and $\Delta_{i\mu}$ is the difference between the rest energies of the initial $\left(\frac{A_1}{Z}X\right)$ and intermediate $\left(\frac{A_1-1}{Z}X$ and $n\right)$ states.

$$\Delta = \Delta_- + \Delta_+, \quad \Delta_{i\mu} = \Delta_- - \Delta_n \quad (16)$$

with

$$\Delta_- = \Delta_{A_1} - \Delta_{A_1-1} \text{ and } \Delta_+ = \Delta_{A_2} - \Delta_{A_2+1}. \quad (17)$$

Δ_{A_1} , Δ_{A_1-1} , Δ_{A_2} , Δ_{A_2+1} and Δ_n are the energy excesses of the neutral atoms of mass numbers A_1 , $A_1 - 1$, A_2 , $A_2 + 1$ and the neutron, respectively. [21]. The sum of initial kinetic energies (E_i) is neglected in the energy Dirac-delta $\delta(E_f - E_i - \Delta)$ and $\Delta E_{\mu i}$ further on.

Now for the sake of simplicity we reindex the particles. Particle indexed with e is the electron, particle indexed with 1 is initially the nucleus ${}^A_1 X$ (particle 2 in Fig. 1) and finally ${}^{A_1-1}_Z X$ (particle 2' in Fig. 1), particle indexed with 2 is initially the nucleus ${}^A_2 X$ (particle 4 in Fig. 1) and finally ${}^{A_2+1}_Z X$ (particle 5 in Fig. 1).

$$E_f = E_{fe}(\mathbf{k}_{fe}) + E_{f1}(\mathbf{k}_1) + E_{f2}(\mathbf{k}_2), \quad (18)$$

$$E_\mu = E_{fe}(\mathbf{k}_{fe}) + E_{\mu 1}(\mathbf{k}_1) + E_n(\mathbf{k}_n), \quad (19)$$

where

$$E_{fj}(\mathbf{k}_j) = \frac{\hbar^2 \mathbf{k}_j^2}{2m_j} \quad (20)$$

is the kinetic energy, $\mathbf{k}_{fj} \equiv \mathbf{k}_j$ is the wave vector and m_j is the rest mass of particle indexed with j in the final state ($j = 1, 2$).

$$E_n(\mathbf{k}_n) = \frac{\hbar^2 \mathbf{k}_n^2}{2m_n} \quad (21)$$

is the kinetic energy, \mathbf{k}_n is the wave vector in the intermediate state and m_n is the rest mass of the neutron. $E_{\mu 1}(\mathbf{k}_1)$ is the kinetic energy of the first particle in the intermediate state, and $E_{\mu 1}(\mathbf{k}_1) = E_{f1}(\mathbf{k}_1)$. The kinetic energy of the electron in the initial and final state

$$E_{ie} = \frac{\hbar^2 \mathbf{k}_{ie}^2}{2m_e} \text{ and } E_{fe} = \frac{\hbar^2 \mathbf{k}_{fe}^2}{2m_e} \quad (22)$$

with \mathbf{k}_{ie} and \mathbf{k}_{fe} denoting the wave vector of the electron in the initial and final state. The initial wave vectors \mathbf{k}_{i1} and \mathbf{k}_{i2} of particles 1 and 2 are neglected. The initial, intermediate and final states are determined in Appendix A., the $V_{\mu i}^{Cb}$, $V_{f\mu}^{St}$ matrix-elements are calculated in Appendix B. and the transition probability per unit time is calculated in Appendix C.. (Appendix D. is devoted to the approximations, identities and relations which are used in the calculation of the cross section.)

A. Cross section of electron assisted neutron exchange process

The cross section σ of the process can be obtained from the transition probability per unit time (77) dividing it

by the flux v_e/V of the incoming electron where v_e is the velocity of the electron.

$$\sigma = \int \frac{c}{v_e} \frac{64\pi^3 \alpha_f^2 \hbar c Z^2 \sum_{l_2=-m_2}^{l_2=m_2} |F_2(\mathbf{k}_2)|^2}{v_c (|\mathbf{k}_1 + \mathbf{k}_2|^2 + \lambda^2)^2 (\Delta E_{\mu i})_{\mathbf{k}_n=\mathbf{k}_2}^2} \times \frac{F_e(E_{ie})}{F_e(E_{f1})} \langle |F_1(\mathbf{k}_2)|^2 \rangle A_2^2 r_{A_2} \delta(E_f - \Delta) d^3 k_1 d^3 k_2, \quad (23)$$

where v_c is the volume of elementary cell in the solid, r_{A_2} is the relative natural abundance of atoms ${}^A_2 X$,

$$F_1(\mathbf{k}_2) = \int \Phi_{i1}(\mathbf{r}_{n1}) e^{-i\mathbf{k}_2 \cdot \frac{A_1}{A_1-1} \cdot \mathbf{r}_{n1}} d^3 r_{n1}, \quad (24)$$

$$\langle |F_1(\mathbf{k}_2)|^2 \rangle = \frac{1}{2l_1 + 1} \sum_{l_1=-m_1}^{l_1=m_1} |F_1(\mathbf{k}_2)|^2 \quad (25)$$

and

$$F_2(\mathbf{k}_2) = \int \Phi_{f2}^*(\mathbf{r}_{n2}) e^{i\mathbf{k}_2 \cdot \mathbf{r}_{n2}} \times \left(-f \frac{\exp(-s \frac{A_2+1}{A_2} r_{n2})}{\frac{A_2+1}{A_2} r_{n2}} \right) d^3 r_{n2}. \quad (26)$$

Here Φ_{i1} and Φ_{f2} are the initial and final bound neutron states (for the definition of l_1 and l_2 see below). The cross section calculation result that the $k_2 \simeq k_0 = \sqrt{2\mu_{12}\Delta}/\hbar$ substitution may be used (see in Appendix D.) in calculating F_1 and F_2 in σ , where $\mu_{12} = m_0 [(A_1 - 1)(A_2 + 1)] / (A_1 + A_2)$.

When evaluating (23) first the Weisskopf approximation is applied, i.e. for the initial and final bound neutron states we take $\Phi_W(\mathbf{r}_{nj}) = \phi_{jW}(r_{nj}) Y_{l_j m_j}(\Omega_j)$, $j = 1, 2$ where $Y_{l_j m_j}(\Omega_j)$ is a spherical harmonics and $\phi_{jW}(r_{nj}) = \sqrt{3/R_j^3}$, $j = 1, 2$ if $|\mathbf{r}_{nj}| \leq R_j$ and $\phi_{jW}(r_{nj}) = 0$ for $|\mathbf{r}_{nj}| > R_j$, where $R_j = r_0 A_j^{1/3}$ is the radius of a nucleus of nucleon number A_j with $r_0 = 1.2 \times 10^{-13}$ cm. We apply the $A_1 \simeq A_2 \simeq A_1 - 1 \simeq A_2 + 1 = A$ approximation further on. Calculating $F_1(\mathbf{k}_0)$ and $F_2(\mathbf{k}_0)$ the long wavelength approximations (LWA) ($\exp(-i\mathbf{k}_0 \cdot \mathbf{r}_{n1}) = 1$ and $\exp(i\mathbf{k}_0 \cdot \mathbf{r}_{n2}) = 1$) are also used with $s = 1/r_0$ that result approximately

$$\langle |F_1(\mathbf{k}_0)|^2 \rangle \sum_{l_2=-m_2}^{l_2=m_2} |F_2(\mathbf{k}_0)|^2 = 16\pi^2 r_0^4 f^2 (2l_2 + 1). \quad (27)$$

Using the results of Appendix D., the $E_{f1} = \Delta/2$ relation and if $E_e < 0.1$ MeV (i.e. if $F_e(E_{ie}) = |2\pi\eta_e(E_{ie})| = 2\pi Z\alpha_f \sqrt{m_e c^2 / 2E_{ie}}$) then the cross section in the Weisskopf-LWA approximation reads as

$$\sigma_W = \frac{C_{W0} (2l_2 + 1)}{\left[1 + \frac{2(\Delta_n - \Delta_-)}{A\Delta}\right]^2} \frac{r_{A_2}}{F_e(\Delta/2)} \frac{A^{3/2} Z^2}{\Delta^{3/2} E_{ie}} \quad (28)$$

with $C_{W0} = 2^{15}\pi^9\alpha_f^3(0.08)^2 a_B r_0 \left(\frac{r_0}{d}\right)^3 (m_0 c^2)^{3/2} m_e c^2$. Here a_B is the Bohr-radius, the relation $c/v_e = \sqrt{m_e c^2 / (2E_{ie})}$ with E_{ie} the kinetic energy of the incoming electrons is also applied and $d = 3.52 \times 10^{-8}$ cm (*Ni* lattice) and $d = 3.89 \times 10^{-8}$ cm (*Pd* lattice). $F_e(\Delta/2)$ is determined by (7) and (8). The subscript W refers to the Weisskopf-LWA approximation and in (28) the quantities Δ and E_{ie} have to be substituted in *MeV* units. $C_{W0}(Ni) = 8.9 \times 10^{-10}$ *MeV*^{5/2}*b* and $C_{W0}(Pd) = 6.6 \times 10^{-10}$ *MeV*^{5/2}*b*.

We have calculated $\sum_{l_2=-m_2}^{l_2=m_2} |F_2(\mathbf{k}_0)|^2$, $\langle |F_1(\mathbf{k}_0)|^2 \rangle$ and the cross section in the single particle shell model with isotropic harmonic oscillator potential and without the long wavelength approximation (see Appendix E.). We introduce the ratio

$$\eta = \frac{\langle |F_1(\mathbf{k}_0)|^2 \rangle_{Sh} \sum_{l_2=-m_2}^{l_2=m_2} |F_2(\mathbf{k}_0)|_{Sh}^2}{\langle |F_1(\mathbf{k}_0)|^2 \rangle_W \sum_{l_2=-m_2}^{l_2=m_2} |F_2(\mathbf{k}_0)|_W^2}. \quad (29)$$

(The subscript *Sh* refers to the shell model.) With the aid of $\eta \equiv \eta_{l_1, n_1, l_2, n_2}(A_1, A_2)$ given by (95) (see Appendix E.) the cross section σ_{Sh} calculated in the shell model can be written as

$$\sigma_{Sh} = \eta_{l_1, n_1, l_2, n_2}(A_1, A_2) \sigma_W. \quad (30)$$

B. Yield of events of electron assisted neutron exchange process

The yield dN/dt of events of electron assisted neutron exchange process $A_1, A_2 \rightarrow A_1 - 1, A_2 + 1$ can be written as

$$\frac{dN}{dt} = N_t N_{ni} \sigma \Phi, \quad (31)$$

where $\sigma = \{\sigma_W \text{ or } \sigma_{Sh}\}$, Φ is the flux of electrons, N_t is the number of target particles, i.e. the number N_{A_1} of irradiated atoms of mass number A_1 in the metal. The contribution of N_{ni} neutrons in each nucleus ${}^A_1 X$ is also taken into account. N_{ni} is the number of neutrons in the uppermost energy level of the initial nucleus ${}^A_1 X$. If F and D are the irradiated surface and the width of the sample, respectively, then the number of elementary cells N_c in the sample is $N_c = FD/v_c = 4FD/d^3$ in the case of *Ni* and *Pd*, and the number of atoms in the elementary cell is $2r_{A_1}$ with r_{A_1} the relative natural abundance of atoms ${}^A_1 X$ thus the number N_t of target atoms of mass number A_1 in the process is

$$N_t = \frac{8}{d^3} r_{A_1} F D. \quad (32)$$

The wave numbers and energies of the two outgoing heavy particles are approximately $\mathbf{k}_1 = -\mathbf{k}_2$,

$$E_1 = \frac{A_2 + 1}{A_1 + A_2} \Delta \text{ and } E_2 = \frac{A_1 - 1}{A_1 + A_2} \Delta. \quad (33)$$

A	58	60	61	62	64
Δ_-	-4.147	-3.317	0.251	-2.526	-1.587
Δ_+	0.928	-0.251	2.526	-1.234	-1.973
r_A	0.68077	0.26223	0.0114	0.03634	0.00926

TABLE I: Numerical data of the $e + {}^{A_1}_{28}Ni + {}^{A_2}_{28}Ni \rightarrow e' + {}^{A_1-1}_{28}Ni + {}^{A_2+1}_{28}Ni + \Delta$ reaction. The reaction is energetically allowed if $\Delta = \Delta_-(A_1) + \Delta_+(A_2) > 0$ holds. A is the mass number, r_A is the relative natural abundance, $\Delta_-(A) = \Delta_A - \Delta_{A-1}$ and $\Delta_+(A) = \Delta_A - \Delta_{A+1}$ are given in *MeV* units.

A	102	104	105	106	108	110
Δ_-	-2.497	-1.912	0.978	-1.491	-1.149	-0.747
Δ_+	-0.446	-0.978	1.491	-1.533	-1.918	-2.320
r_A	0.0102	0.1114	0.2233	0.2733	0.2646	0.1172

TABLE II: Numerical data of the $e + {}^{A_1}_{46}Pd + {}^{A_2}_{46}Pd \rightarrow e' + {}^{A_1-1}_{46}Pd + {}^{A_2+1}_{46}Pd + \Delta$ reaction. The reaction is energetically allowed if $\Delta = \Delta_-(A_1) + \Delta_+(A_2) > 0$ holds. A is the mass number, r_A is the relative natural abundance, $\Delta_-(A) = \Delta_A - \Delta_{A-1}$ and $\Delta_+(A) = \Delta_A - \Delta_{A+1}$ are given in *MeV* units.

C. Numerical data of electron assisted neutron exchange processes in *Ni* and *Pd*

As a first example we take *Ni* as target material. In this case the possible processes are

$$e + {}^{A_1}_{28}Ni + {}^{A_2}_{28}Ni \rightarrow e' + {}^{A_1-1}_{28}Ni + {}^{A_2+1}_{28}Ni + \Delta. \quad (34)$$

Tables I. and III. contain the relevant data for reaction (34). Describing neutrons in the uppermost energy level of ${}^A_{28}Ni$ isotopes we used *1p* shell model states in the cases of $A = 58 - 60$ and *0f* shell model states in the cases of $A = 61 - 64$.

Another interesting target material is *Pd* in which the electron assisted neutron exchange processes are the

$$e + {}^{A_1}_{46}Pd + {}^{A_2}_{46}Pd \rightarrow e' + {}^{A_1-1}_{46}Pd + {}^{A_2+1}_{46}Pd + \Delta \quad (35)$$

reactions. The relevant data can be found in Tables II. and IV.. Describing neutrons in the uppermost energy level of ${}^A_{46}Pd$ isotopes we used *0g* shell model states in the cases of $A = 102 - 104$ and *1d* shell

$A_1 \rightarrow A_1 - 1$	$A_2 \rightarrow A_2 + 1$	$\Delta(\text{MeV})$	η
61 \rightarrow 60	58 \rightarrow 59	1.179	7.02×10^{-3}
61 \rightarrow 60	61 \rightarrow 62	2.777	2.42×10^{-8}
64 \rightarrow 63	61 \rightarrow 62	0.939	2.08×10^{-4}

TABLE III: The values of the quantities η and $\Delta = \Delta_-(A_1) + \Delta_+(A_2) > 0$, the later in *MeV* units, of the $e + {}^{A_1}_{28}Ni + {}^{A_2}_{28}Ni \rightarrow e' + {}^{A_1-1}_{28}Ni + {}^{A_2+1}_{28}Ni + \Delta$ reaction. The $\Delta_-(A_1)$ and $\Delta_+(A_2)$ values can be found in Table I. For the definition of η see (29) and (95).

$A_1 \rightarrow A_1 - 1$	$A_2 \rightarrow A_2 + 1$	$\Delta(\text{MeV})$	η
105 \rightarrow 104	102 \rightarrow 103	0.532	1.84×10^{-4}
105 \rightarrow 104	105 \rightarrow 106	2.469	8.88×10^{-11}
108 \rightarrow 107	105 \rightarrow 106	0.342	2.82×10^{-3}

TABLE IV: The values of the quantities η and $\Delta = \Delta_-(A_1) + \Delta_+(A_2) > 0$, the later in *MeV* units, of the $e + {}^{A_1}_{46}\text{Pd} + {}^{A_2}_{46}\text{Pd} \rightarrow e' + {}^{A_1-1}_{46}\text{Pd} + {}^{A_2+1}_{46}\text{Pd} + \Delta$ reaction. The $\Delta_-(A_1)$ and $\Delta_+(A_2)$ values can be found in Table II. For the definition of η see (29) and (95).

model states in the cases of $A = 105 - 108$. The nuclear data to the Tables are taken from [21]. One can see from Tables III. and IV. that in both cases three possible pairs of isotopes exist which are energetically allowed (for which $\Delta > 0$) and their rates differ in the factor $(2l_2 + 1) N_{ni} \eta_{l_1, n_1, l_2, n_2}(A_1, A_2) r_{A_1} r_{A_2} \Delta^{-3/2}$ only. The $\eta \equiv \eta_{l_1, n_1, l_2, n_2}(A_1, A_2)$ values of *Ni* and *Pd* can also be found in Tables III. and IV., respectively. The results of numerical investigation of $(2l_2 + 1) N_{ni} \eta_{l_1, n_1, l_2, n_2}(A_1, A_2) r_{A_1} r_{A_2} \Delta^{-3/2}$ shows that the 61 \rightarrow 60, 58 \rightarrow 59 and the 108 \rightarrow 107, 105 \rightarrow 106 reactions are the dominant among the processes in *Ni* and *Pd*, respectively.

In the case of *Ni* it is found that the

$$e + {}^{61}_{28}\text{Ni} + {}^{58}_{28}\text{Ni} \rightarrow e' + {}^{60}_{28}\text{Ni} + {}^{59}_{28}\text{Ni} + 1.179 \text{ MeV} \quad (36)$$

process of $\sigma_{Sh} = 0.54/E_{ie} \text{ mb}$ with E_{ie} in *MeV* is leading. In this case the ${}^{60}_{28}\text{Ni}$ and the ${}^{59}_{28}\text{Ni}$ isotopes take away 0.585 *MeV* and 0.594 *MeV*, respectively. In the case of *Pd* the

$$e + {}^{108}_{46}\text{Pd} + {}^{105}_{46}\text{Pd} \rightarrow e' + {}^{107}_{46}\text{Pd} + {}^{106}_{46}\text{Pd} + 0.342 \text{ MeV} \quad (37)$$

reaction of $\sigma_{Sh} = 1.6/E_{ie} \text{ mb}$ with E_{ie} in *MeV* is found to be the leading one. In this case the ${}^{107}_{46}\text{Pd}$ and the ${}^{106}_{46}\text{Pd}$ isotopes take away 0.170 *MeV* and 0.172 *MeV*, respectively.

III. OTHER RESULTS - OTHER CHARGED PARTICLE ASSISTED REACTIONS

The transition probability per unit time and the cross section of the processes, which will be discussed below, may be determined in similar manner as was done above in the case of electron assisted neutron exchange process. The main difference is that in matrix elements $V_{\mu i}^{Cb}$ and $V_{f\mu}^{St}$ different Coulomb factors appear according to the particles which take part in the reaction.

A. Electron assisted heavy charged particle exchange process

There is an other possibility in the family of electron assisted exchange processes, when a charged heavy par-

ticle (such as p , d , t , ${}^3_2\text{He}$ and ${}^4_2\text{He}$) is exchanged. The process is called electron assisted heavy charged particle exchange process and it can be visualized with the aid of Fig.1 too. Denoting the intermediate particle (particle 3 in Fig. 1) by ${}^{A_3}_{z_3}w$, which is exchanged, the general electron assisted heavy charged particle exchange processes reads as

$$e + {}^{A_1}_{Z_1}X + {}^{A_2}_{Z_2}Y \rightarrow e' + {}^{A_1-A_3}_{Z_1-z_3}X^* + {}^{A_2+A_3}_{Z_2+z_3}Y^* + \Delta. \quad (38)$$

Here e and e' denote electron and Δ is the energy of the reaction, i.e. the difference between the rest energies of initial $({}^{A_1}_{Z_1}X + {}^{A_2}_{Z_2}Y)$ and final $({}^{A_1-A_3}_{Z_1-z_3}X^* + {}^{A_2+A_3}_{Z_2+z_3}Y^*)$ states. $\Delta = \Delta_- + \Delta_+$, with $\Delta_- = \Delta_{Z_1}^{A_1} - \Delta_{Z_1-z_3}^{A_1-A_3}$ and $\Delta_+ = \Delta_{Z_2}^{A_2} - \Delta_{Z_2+z_3}^{A_2+A_3}$. $\Delta_{Z_1}^{A_1}$, $\Delta_{Z_1-z_3}^{A_1-A_3}$, $\Delta_{Z_2}^{A_2}$, $\Delta_{Z_2+z_3}^{A_2+A_3}$ are the energy excesses of neutral atoms of mass number-charge number pairs A_1, Z_1 ; $A_1 - A_3, Z_1 - z_3$; A_2, Z_2 ; $A_2 + A_3, Z_2 + z_3$, respectively [21].

In (38) the electron (particle 1) Coulomb interacts with the nucleus ${}^{A_1}_{Z_1}X$ (particle 2). A scattered electron (particle 1'), the intermediate particle ${}^{A_3}_{z_3}w$ (particle 3) and the nucleus ${}^{A_1-A_3}_{Z_1-z_3}X^*$ (particle 2') are created due to this interaction. The intermediate particle ${}^{A_3}_{z_3}w$ (particle 3) is captured due to the strong interaction by the nucleus ${}^{A_2}_{Z_2}Y$ (particle 4) forming the nucleus ${}^{A_2+A_3}_{Z_2+z_3}Y^*$ (particle 5) in this manner. So in (38) the nucleus ${}^{A_1}_{Z_1}X$ (particle 2) loses a particle ${}^{A_3}_{z_3}w$ which is taken up by the nucleus ${}^{A_2}_{Z_2}Y$ (particle 4). The process is energetically forbidden if $\Delta < 0$. Since particles 2', 3 and 4 all have positive charge, furthermore they all are heavy, the two Coulomb factors, which appear in the cross section, are $F_{2'3}$ and F_{34} . Therefore the cross section of process (38) is expected to be much smaller than the cross section of process (9). However process (38) may play an essential role in explaining nuclear transmutations stated [3] (see below). Since Coulomb factors $F_{2'3}$ and F_{34} determine the order of magnitude of the cross section of the process (the cross section of the process is proportional to $F_{2'3}F_{34}$) we treat them in more detail in Appendix F.

B. Electron assisted nuclear capture process

Now the electron assisted nuclear capture process (see Fig. 2) is considered, in which an electron-nucleus Coulomb scattering is followed by a capture process governed by strong interaction [17]. When describing the effect of the Coulomb interaction between the nucleus of charge number Z and a slow electron one can also use the Coulomb factor $F_e(E)$ (7) of the electron defined above.

As an example we consider the electron assisted $d+d \rightarrow {}^4_2\text{He}$ process with slow deuterons. In this case, one of the slow deuterons (as particle 2) can enter into Coulomb interaction with a quasi-free, slow electron (as particle 1) of the solid (see Fig. 2). In Coulomb scattering of free deuterons and electrons the wave number vector (momentum) is preserved since their relative mo-

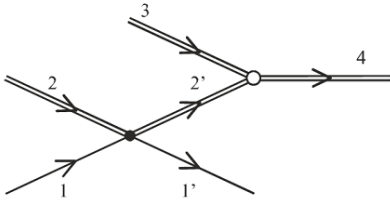


FIG. 2: The graph of electron assisted nuclear capture reactions. The simple lines represent free (initial (1) and final (1')) electrons. The doubled lines represent free, heavy, charged initial (2) particles (such as p, d), their intermediate state (2'), target nuclei (3) and reaction product (4). The filled dot denotes Coulomb-interaction and the open circle denotes nuclear (strong) interaction.

tion may be described by a plane wave which is multiplied by the corresponding Coulomb factor. In this second order process the Coulomb interaction is followed by strong interaction, which induces a nuclear capture process. The energy Δ of the nuclear reaction is divided between the electron and the heavy nuclear product. Since $m_N \gg m_e$ (m_N is the rest mass of the nuclear product), the electron will take almost all the total nuclear reaction energy Δ away (there is no gamma emission) and the magnitude $k_{1'}$ of its wave number vector $\mathbf{k}_{1'}$ reads $k_{1'} = \sqrt{\Delta^2 + 2m_e c^2 \Delta} / (\hbar c) \simeq \Delta / (\hbar c)$ (if $\Delta \gg m_e c^2$). If initially the electron and the deuteron move slowly and the magnitudes of their wave number vectors are much smaller than $\Delta / (\hbar c)$, then the initial wave number vectors can be neglected in the wave number vector (momentum) conservation and consequently, in the intermediate state (in state 2') the deuteron gets a wave number vector $\mathbf{k}_{2'} = -\mathbf{k}_{1'}$. If $\Delta = 23.84 \text{ MeV}$, which is the reaction energy of the $d + d \rightarrow {}^4_2\text{He}$ reaction, then the deuteron 2' will have $k_{2'} = \Delta / (\hbar c)$ and its corresponding (virtual) kinetic energy $E_{2'} = \Delta^2 / (4m_0 c^2) = 76.5 \text{ keV}$ in the CM coordinate system. At this energy the Coulomb factor value between particles 2' and 3 reads as $F_{2'3} = 0.103$. It must be compared to the extremely small Coulomb factor value, e.g. in the case of energy $E = 1 \text{ eV}$ to $F_{23}(1 \text{ eV}) = 1.1 \times 10^{-427}$, that is characteristic of the usual, first order process. If one compares again the cross sections of second order and first order (electron assisted and usual) processes then their ratio is approximately proportional to $F_e F_{2'3} / F_{23}(E)$ that becomes extremely large with decreasing E too. (The model and the details of calculation, the results and their discussion can be found in [17].) The cross section of the electron assisted neutron exchange process is expected to be larger than the cross section of electron assisted nuclear capture process because of the appearance of the Coulomb factor in it.

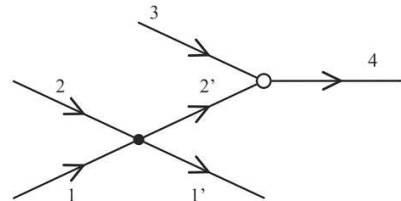


FIG. 3: The graph of heavy particle assisted nuclear capture reactions. The lines 1, 1' represent free (initial (1) and final (1')) heavy particle which assists the reaction. The other lines represent heavy, charged initial (2) particles, their intermediate state (2'), target nuclei (3) and reaction product (4). The filled dot denotes Coulomb-interaction and the open circle denotes nuclear (strong) interaction.

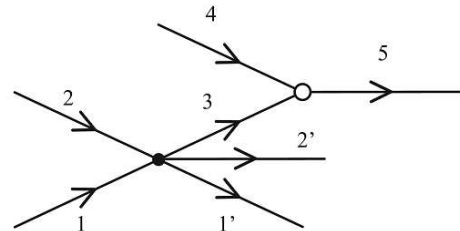


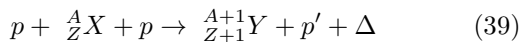
FIG. 4: The graph of heavy particle assisted heavy charged particle (such as p, d, t, ${}^3_2\text{He}$ and ${}^4_2\text{He}$) exchange reaction. The lines 1, 1' represent free (initial (1) and final (1')) heavy particle which assists the reaction. The other lines represent heavy, charged initial nuclei (2), their final state (2', which is a nucleus lost particle 3), the transferred particle (3), target nuclei (4) and reaction product (5). The filled dot denotes Coulomb-interaction and the open circle denotes nuclear (strong) interaction.

C. Heavy particle assisted nuclear processes

In electron assisted nuclear reactions heavy, charged particles of energy of a few MeV may be created. In the decelerating process of reaction products of the electron assisted processes the energy of these heavy particles may become intermediately low (of about $0.01 [MeV]$) so their Coulomb factor, if the particles are light, may be intermediately small so their assistance in nuclear processes have to be also considered among the accountable nuclear processes. The corresponding graphs can be seen in Fig. 3 and Fig. 4. Fig. 3 depicts a heavy, charged particle assisted nuclear capture process and Fig. 4 represents heavy, charged particle assisted heavy charged particle (such as p, d, t, ${}^3_2\text{He}$ and ${}^4_2\text{He}$) exchange reaction. Now all particles are heavy. According to the applied notation, particles 2', 3 (in Fig. 3) and particles 3, 4 (in Fig. 4) take part in a nuclear process and particle 1 only assists it. The different processes will be distinguished by the type of the assisting particle and also by the type of the nuclear process. In our model charged, heavy particles, such as protons (p), deuterons (d) may be particle

1, which are supposed to move freely in a solid (e.g. in a metal). The other particles, that may take part in the processes are: localized heavy, charged particles (bound, localized p , d and other nuclei) as the participants of Coulomb scattering (with particle 1) and localized heavy, charged particles (bound, localized p , d and other nuclei) as nuclear targets (as particle 3 in Fig. 3 and particle 4 in Fig. 4). The problem, that there may be identical particles in the system that are indistinguishable, is also disregarded here.

The calculation of the transition probability per unit time of the process can be performed through similar steps to those applied for the calculation of the rate of an electron assisted process. The main difference is that now particle 1 is heavy. In order to show the capability of the heavy particle assisted nuclear processes, some cases of the proton assisted proton captures



were investigated in Appendix III. (Ch. IX.) of [17].

IV. DISCUSSION - ANALYSIS OF EXPERIMENTAL OBSERVATIONS

A. Anomalous screening effect

Recently the electron assisted low energy dd reactions were investigated in solids [18]. It was shown that if deuterized metal is irradiated with slow, free deuterons then the $e + d + d \rightarrow e' + p + t$ and $e + d + d \rightarrow e' + n + {}^3He$ electron assisted dd processes have measurable probabilities even in the case of slow deuterons. (The electron assisted $d + d \rightarrow p + t$ and $d + d \rightarrow n + {}^3He$ reactions are electron assisted neutron and proton exchange processes, respectively. In these processes electrons of the conduction band of metals, which may be considered quasi-free, assist the reaction.) The cross sections and the yields in an irradiated sample were also determined. The cross sections σ_{pt} and σ_{nHe} of the electron assisted $d + d \rightarrow p + t$ and $d + d \rightarrow n + {}^3He$ reactions read as $\sigma_{pt} = uC_{pt}/E$ and $\sigma_{nHe} = uC_{nHe}/E$, respectively, with E the kinetic energy of the deuterons in the beam (in MeV units) and u the deuteron over metal number densities in the target. We have obtained $C_{pt} = 2.32 \times 10^{-8} MeVb$ and $C_{nHe} = 1.82 \times 10^{-8} MeVb$ in the case of deuterized Pd . We are going to compare our cross section result with the cross sections of the usual $d(d, n){}^3He$ and $d(d, p)t$ reactions.

The energy dependence of the cross section (σ) of the usual charged-particle induced reactions reads as

$$\sigma(E) = S(E) \exp[-2\pi\eta_{jk}(E)]/E, \quad (40)$$

where $S(E) = S(0) + S_1E + S_2E^2$ is the astrophysical factor [4]. In the low energy range the $S(E) = S(0)$ approximation is valid. The $\exp[-2\pi\eta_{jk}(E)]$ dependence originates from the Coulomb factor, thus the $S(0)/E$ part

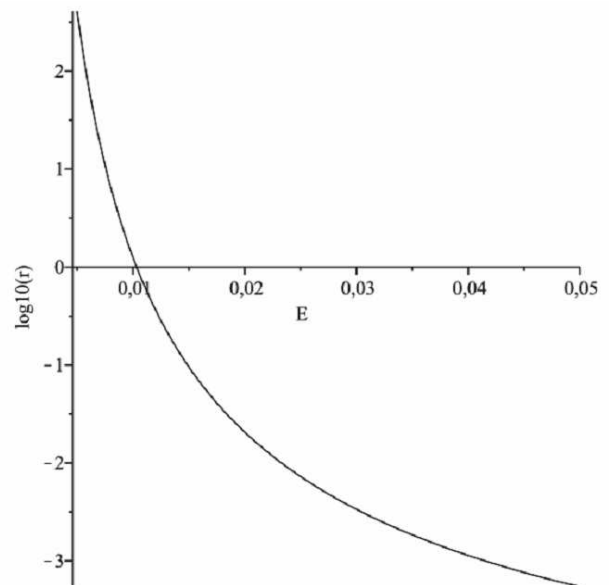


FIG. 5: The beam energy (E) dependence of $\log_{10}(r)$ in the case of Pd . The relative yield r is the ratio of the rates of electron assisted and normal $d + d \rightarrow p + t$ processes in an elementary volume of the sample.

of the cross section is worth comparing to our results, especially the $S(0)$ values to the C_{pt} and C_{nHe} values obtained by us. The $S(0)$ values of processes $d(d, n){}^3He$ and $d(d, p)t$ are: $0.055 MeVb$ and $0.056 MeVb$, respectively [4]. On the basis of these numbers we can also say that our result seems to be reasonable.

It is useful to introduce the relative yield

$$r = \frac{\left(\frac{dN}{dt}\right)_{pt}}{\left(\frac{dN}{dt}\right)_{usual}} = \frac{g_e C_{pt}}{2N_c S(0)} \exp[2\pi\eta(E)], \quad (41)$$

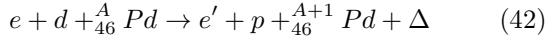
which is the ratio of the yields of electron assisted $\left[\left(\frac{dN}{dt}\right)_{pt}\right]$ and normal $\left[\left(\frac{dN}{dt}\right)_{usual}\right]$ $d + d \rightarrow p + t$ processes in an elementary volume of the sample. Here N_c is the number of atoms in the elementary cell and g_e is the number of conduction electrons in an elementary cell. The results were connected with the so called anomalous screening effect [13].

In the case of deuterized Pd we have got $r = 1.04 \times 10^{-6} \exp[2\pi\eta(E)]$ where $\eta(E) = \alpha_f \sqrt{m_0 c^2 / E}$ resulting $r = 5.43 \times 10^{-4}$ at $E = 0.05 MeV$ and $r = 409$ at $E = 0.005 MeV$ (the energy interval $0.005 MeV < E < 0.05 MeV$ was investigated in [13]) and $r = 1.006$ at $E = 0.01031 MeV$. For $E < 0.023$ the relative yield is larger than 1%. The energy dependence of $\log_{10}(r)$ can be seen in Fig. 5. From these data and from Fig. 5 one can see that the yield produced by the electron assisted $d + d \rightarrow p + t$ process with decreasing beam energy becomes comparable to and larger than the yield produced by the normal $d + d \rightarrow p + t$ process. Since $C_{nHe} = 1.82 \times 10^{-8} MeVb$ therefore σ_{nHe} has the same

order of magnitude as that of σ_{pt} and so similar statement can be made in the case of electron assisted $d + d \rightarrow n + {}^3\text{He}$ reaction too. Consequently, one can conclude that the electron assisted $d + d \rightarrow p + t$ and $d + d \rightarrow n + {}^3\text{He}$ processes should be taken into account when evaluating the data [13] of low energy fusion reactions in metals.

B. Fleischmann-Pons experiment

In the experiment of [1] Pd was filled with deuterons during electrolysis. The electrolyte had $LiOD$ content too. Two types of electron assisted neutron exchange processes with Pd nuclei are possible:

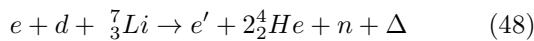
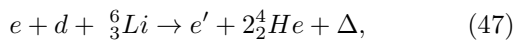
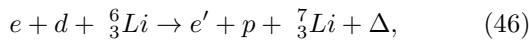
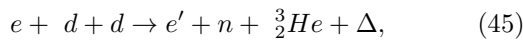
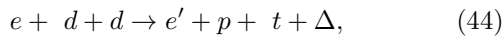


with $\Delta = \Delta_-(d) + \Delta_+(A)$ and

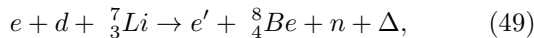


with $\Delta = \Delta_-(Li) + \Delta_+(A)$ (the $\Delta_+(A)$ values can be found in Table III). $\Delta_-(d) = \Delta_d - \Delta_p = 5.847 \text{ MeV}$ and $\Delta_-(Li) = \Delta({}_3^7Li) - \Delta({}_3^6Li) = 0.821 \text{ MeV}$ are the energies of neutron loss of d and ${}_3^7Li$, where Δ_d , Δ_p , $\Delta({}_3^7Li)$ and $\Delta({}_3^6Li)$ are the mass excesses of deuteron, proton, ${}_3^7Li$ and ${}_3^6Li$, respectively. In reactions (42) and (43) electrons of the metal are particle 1, d and ${}_3^7Li$ are particle 2 and ${}^{46}_APd$ appears as particle 4 (see Fig. 1). Reaction (42) is energetically allowed for all the natural isotopes of Pd since $\Delta = \Delta_-(d) + \Delta_+(A) > 0$ for each A (see the $\Delta_+(A)$ values of Table II). In the case of reaction (43) the $\Delta = \Delta_-(Li) + \Delta_+(A) > 0$ condition holds at $A = 102$ and $A = 105$ resulting $\Delta = 0.375 \text{ MeV}$ and $\Delta = 2.312 \text{ MeV}$, respectively.

However, at the Pd surface other types of electron assisted neutron exchange processes with d and Li nuclei of the electrolyte and d solved in Pd are possible:

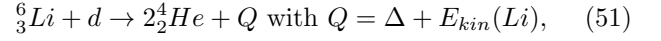
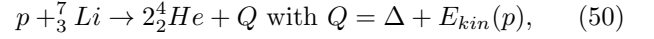


and

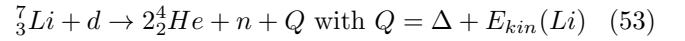


which is promptly followed by the decay ${}^8_4Be \rightarrow 2{}_2^4He$ ($\Gamma_\alpha = 6.8 \text{ eV}$). In these reactions electrons of the metal are particle 1 and d is particle 2.

In reaction (42) protons of energy up to 7.269 MeV and in reaction (43) ${}_3^6Li$ particles of maximum energy 2.189 MeV are created which may enter into usual nuclear reactions with the nuclei of deuteron loaded Pd and electrolyte which are (without completeness): the usual $pd \rightarrow {}_2^3He + \gamma$ reaction,



In (50) and (51) the emitted ${}_2^4He$ has energy $E_{4He} > 8.674 \text{ MeV}$ and $E_{4He} > 11.186 \text{ MeV}$, and in (52) the created p and ${}_3^7Li$ have energy $E_p > 4.397 \text{ MeV}$ and $E_{7Li} > 0.628 \text{ MeV}$, respectively. It can be seen that in (50) and (51) ${}_2^4He$ is produced. The ${}_3^7Li$ particles may enter into reaction



which contributes to the ${}_2^4He$ production too. Here and above $E_{kin}(p)$ and $E_{kin}(Li)$ are the kinetic energies of the initial protons, ${}_3^6Li$ and ${}_3^7Li$ isotopes.

From the above one can see that at least twelve types of reactions (altogether 18 reactions) exist which are capable of energy production and in half of them energy production is accompanied with ${}_2^4He$ production. It is reasonable that reactions (42) and (43) have the highest rate in the above list of reactions. In the majority of the above reactions charged particles, mostly heavy charged particles are created with short range and so they lose their energy in the matter of the experimental apparatus mainly in the electrode (cathode) and the electrolyte, therefore their direct observation is difficult. It is mainly heat production, which is a consequence of deceleration in the matter of the apparatus, that can be experienced. The third of the processes, mainly the secondary processes are the sources of neutron emission. X- and γ -rays may be originated mainly from bremsstrahlung. The above reasoning tallies with experimental observations.

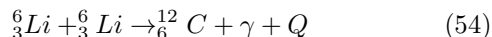
In reactions (42) – (53) heavy, charged particles of kinetic energy lying in the MeV range are created which are able to assist nuclear reactions. One can obtain the possible heavy charged particles assisted reactions if in reactions (42) – (49) the electron is replaced by heavy charged particles (p , t , ${}_2^3He$, ${}_2^4He$, ${}_3^6Li$, ${}_3^7Li$, ${}_4^8Be$ and ${}^{A+1}_{46}Pd$ with $A = 102, 104 - 106, 108, 110$) which are created in reactions (42) – (53). Since the number of possible heavy charged particles is 13 and the number of reactions which may be assisted by them is 8, at least 104 heavy charged particle assisted reactions must be taken into account. Consequently, it is a rather great theoretical challenge and task to determine precisely the relative rates and their couplings of all the accountable reactions,

a work which is, nevertheless, necessary for the accurate quantitative analysis of experiments.

The relative rates of coupled reactions of many types depend significantly on the geometry, the kind of matter and other parameters of the experimental apparatus and on some further variables, which may be attached to a concrete experiment. This situation may be responsible for the diversity of the results of experiments, which are thought to have been carried out with seemingly in the same circumstances.

C. Nuclear transmutation

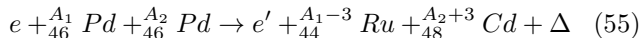
As to the phenomenon of nuclear transmutation [3] we demonstrate its possibility only. First let us see the possibility of normal reactions. For instance in a Fleischmann-type experiment ${}^6_3\text{Li}$ particles of energy up to 2.189 MeV are created in reaction (43) so the reaction



may have minor, but measurable probability. Here $Q = \Delta + E_{kin}(\text{Li})$.

The Coulomb factor of reaction (54) is $F_{Li,Li} = 1.71 \times 10^{-3}$ at 2.189 MeV kinetic energy of ${}^6_3\text{Li}$ particles. The magnitude of the Coulomb factor indicates that the rate of reaction (54) may be large enough to be able to produce carbon traces in observable quantity.

Moreover, in reactions (42) and (43) free ${}^{46}_{46}\text{Pd}$ particles are created offering e.g. the possibility of the



electron assisted ${}^3_2\text{He}$ exchange process. The electron and the other Pd particle are in the solid. Analyzing mass excess data [21] it was found that e.g. the $e + {}^{103}_{46}\text{Pd} + {}^{111}_{46}\text{Pd} \rightarrow e' + {}^{100}_{44}\text{Ru} + {}^{114}_{48}\text{Cd} + \Delta$ ${}^3_2\text{He}$ exchange process has reaction energy $\Delta = 5.7305\text{ MeV}$. [${}^{103}_{46}\text{Pd}$ and ${}^{111}_{46}\text{Pd}$ are produced in reaction (42).] Calculating the $F_{2/3} = F_{3/4}$ Coulomb factors taking $A = 100$, $Z = 46$, $A_3 = 3$, $z_3 = 2$ in (105) one gets $F_{2/3}F_{3/4} = 2.5 \times 10^{-12}$ which seems to be large enough number to produce Cd and Ru traces in an experiment lasting many days long.

The above reactions may offer starting point for the explanation of nuclear transmutations.

D. Rossi-type reactor (E-cat)

Recently the Rossi-type reactor [22] (E-Cat) was experimentally investigated in detail [23]. The fuel contained mostly Ni and also Li in accountable measure, there was 0.011g Li in 1 g fuel. The isotope composition of the unused fuel was equal to the relative natural abundances. But the isotope composition of the ash (the fuel after 32 day run of the reactor) strongly changed. (The measured relative abundances of Li and Ni isotopes in fuel and ash can be seen in Table V. The natural abundances are also given for comparison. The data

Isotope	Fuel	Ash	Natural
${}^6_3\text{Li}$	0.086	0.921	0.075
${}^7_3\text{Li}$	0.914	0.079	0.925
${}^{58}_{28}\text{Ni}$	0.67	0.008	0.681
${}^{60}_{28}\text{Ni}$	0.263	0.005	0.262
${}^{61}_{28}\text{Ni}$	0.019	0.000	0.018
${}^{62}_{28}\text{Ni}$	0.039	0.987	0.036
${}^{64}_{28}\text{Ni}$	0.01	0	0.009

TABLE V: Measured relative abundances of Li and Ni isotopes in fuel and ash. The natural relative abundances are also given for comparison. The data are taken from [23].

are taken from Appendix 3. of [23].) One can see that the ${}^{62}_{28}\text{Ni}$ isotope is enriched and the other Ni isotopes are depleted. Furthermore, the relative ${}^7_3\text{Li}$ content decreased from 0.917 to 0.079 while the relative ${}^6_3\text{Li}$ content increased from 0.086 to 0.921.

The reactor worked for about ten days at temperature $T_1 = 1533\text{ K}$ and the remaining time at temperature $T_2 = 1673\text{ K}$. At these temperatures a free electron gas may be created from the Ni powder of the fuel due to the termionic emission process. The emitted flux of electrons can be determined from the current density of electrons according to the Richardson's law using the work function $U = 5.24\text{ eV}$ of Ni . The obtained termionic electron fluxes are $\Phi_1 = 7.5 \times 10^9\text{ cm}^{-2}\text{s}^{-1}$ and $\Phi_2 = 2.4 \times 10^{11}\text{ cm}^{-2}\text{s}^{-1}$ at T_1 and T_2 , respectively. Regarding the large surface of the powder fuel it is reasonable to suppose that the free electron gas is formed near the surfaces of grains of powder. But if a free electron gas interacts with the $\text{LiAlH}_4 - \text{Ni}$ powder mixture applied then the above observations can be well explained by the electron assisted neutron exchange processes. ${}^7_3\text{Li}$ has $\Delta_- = 0.8214\text{ MeV}$ so it is able to lose neutron. The Δ_+ values of the Ni isotopes can be found in Table I. Completing Table I with $\Delta_+({}^{59}_{28}\text{Ni}) = 3.319\text{ MeV}$ (the half life of ${}^{59}_{28}\text{Ni}$ is $\tau = 7.6 \times 10^4\text{ y}$) one can recognize that the $e + {}^7_3\text{Li} + {}^{A}_{28}\text{Ni} \rightarrow e' + {}^6_3\text{Li} + {}^{A+1}_{28}\text{Ni} + \Delta$ reaction has $\Delta > 0$ value for $A = 58 - 61$ but in the case of $A = 62$ the chain of reactions breaks since in this case $\Delta < 0$ because $\Delta_+({}^{62}_{28}\text{Ni}) = -1.234\text{ MeV}$. The $64 \rightarrow 63$; $61 \rightarrow 62$ reaction of type (34) (see Table III) leads to production of ${}^{63}_{28}\text{Ni}$ ($\tau = 100.1\text{ y}$) which has $\Delta_-({}^{63}_{28}\text{Ni}) = 1.2335\text{ MeV}$ allowing and coupling transition $63 \rightarrow 62$ to transitions $58 \rightarrow 59$; $59 \rightarrow 60$; $60 \rightarrow 61$ and $61 \rightarrow 62$ in reaction (34). These facts explain the enrichment of ${}^{62}_{28}\text{Ni}$ and ${}^6_3\text{Li}$ and the depletion of ${}^7_3\text{Li}$ and Ni isotopes of $A = 58 - 61$ and 64 . (Reactions (34) too contribute to the enrichment of ${}^{62}_{28}\text{Ni}$ (see Table III).)

V. CONCLUSION

It is thought that, in principle, the electron assisted processes are able to answer the questions raised in the

introduction. The exchange of the original, extremely small Coulomb factor to the Coulomb factor of order of unity of the electron in electron assisted processes answers problem (a). The electron assisted nuclear reactions and the reactions which are coupled with them are not accompanied by the expected nuclear end products answering problem (b). Problem (c), the asserted appearance of nuclear transmutations is partly answered in Section IV.C. with the aid of charged particle assisted and usual nuclear reactions.

Summarizing, the theoretical results expounded and their successful applications in explaining some unresolved experimental facts inspire us to say that the studying of charged particles electron assisted nuclear reactions, especially the electron assisted neutron exchange processes may start a renaissance in the field of low energy nuclear physics.

VI. APPENDIX

A. Initial, intermediate and final states of electron assisted neutron exchange process

Let Ψ_i , Ψ_μ and Ψ_f denote the space dependent parts of initial, intermediate and final states, respectively. The initial state has the form

$$\Psi_i(\mathbf{x}_e, \mathbf{x}_1, \mathbf{x}_{n1}, \mathbf{x}_2) = \psi_{ie}(\mathbf{x}_e) \psi_{i1n}(\mathbf{x}_1, \mathbf{x}_{n1}) \psi_{i2}(\mathbf{x}_2), \quad (56)$$

where

$$\psi_{ie}(\mathbf{x}_e) = V^{-1/2} e^{i\mathbf{k}_{ie} \cdot \mathbf{x}_e} \text{ and } \psi_{i2}(\mathbf{x}_2) = V^{-1/2} e^{i\mathbf{k}_{i2} \cdot \mathbf{x}_2} \quad (57)$$

are the initial state of the electron and the nucleus $\frac{A_2}{Z}X$, and $\psi_{i1n}(\mathbf{x}_1, \mathbf{x}_{n1})$ is the initial state of the neutron and the initial $A_1 - 1$ nucleon of the nucleus $\frac{A_1}{Z}X$. $\mathbf{x}_e, \mathbf{x}_1, \mathbf{x}_{n1}$ and \mathbf{x}_2 are the coordinates of the electron, the center of mass of the initial $A_1 - 1$ nucleon, the neutron and the nucleus $\frac{A_2}{Z}X$, respectively. \mathbf{k}_{ie} and \mathbf{k}_{i2} are the initial wave vectors of the electron and the nucleus $\frac{A_2}{Z}X$ and V is the volume of normalization. The initial state $\psi_{i1n}(\mathbf{x}_1, \mathbf{x}_{n1})$ of the neutron and the initial $A_1 - 1$ nucleon may be given in the variables $\mathbf{R}_1, \mathbf{r}_{n1}$

$$\psi_{i1n}(\mathbf{R}_1, \mathbf{r}_{n1}) = V^{-1/2} \exp(i\mathbf{k}_{i1} \cdot \mathbf{R}_1) \Phi_{i1}(\mathbf{r}_{n1}) \quad (58)$$

where \mathbf{R}_1 is the center of mass coordinate of the nucleus $\frac{A_1}{Z}X$ and \mathbf{r}_{n1} is the relative coordinate of one of its neutrons. \mathbf{R}_1 and \mathbf{r}_{n1} are determined by the usual $\mathbf{x}_{n1} = \mathbf{R}_1 + \mathbf{r}_{n1}$ and $\mathbf{R}_1 = [(A_1 - 1)\mathbf{x}_1 + \mathbf{x}_{n1}]/A_1$ relations where \mathbf{x}_{n1} and \mathbf{x}_1 are the coordinates of the neutron and of the center of mass of the initial $A_1 - 1$ nucleon, respectively. The inverse formula for \mathbf{x}_1 is $\mathbf{x}_1 = \mathbf{R}_1 - \mathbf{r}_{n1}/(A_1 - 1)$. In (58) the $\Phi_{i1}(\mathbf{r}_{n1})$ is the wave function of the neutron in the initial bound state of nucleus $\frac{A_1}{Z}X$, \mathbf{k}_{i1} is the initial wave vector of nucleus $\frac{A_1}{Z}X$.

The intermediate state has the form

$$\Psi_\mu(\mathbf{x}_e, \mathbf{x}_1, \mathbf{x}_{n1}, \mathbf{x}_2) = \psi_{fe}(\mathbf{x}_e) \psi_{\mu1n}(\mathbf{x}_1, \mathbf{x}_{n1}) \psi_{i2}(\mathbf{x}_2), \quad (59)$$

where

$$\psi_{fe}(\mathbf{x}_e) = V^{-1/2} e^{i\mathbf{k}_{fe} \cdot \mathbf{x}_e} \quad (60)$$

with \mathbf{k}_{fe} the wave vector of the electron in the final state and $\psi_{i2}(\mathbf{x}_2)$ is given in (57). The state $\psi_{\mu1n}(\mathbf{x}_1, \mathbf{x}_{n1})$ is the product of two plane waves $\psi_{f1}(\mathbf{x}_1) = V^{-1/2} e^{i\mathbf{k}_1 \cdot \mathbf{x}_1}$ and $\psi_n(\mathbf{x}_{n1}) = V^{-1/2} e^{i\mathbf{k}_n \cdot \mathbf{x}_{n1}}$, which are the final state of the nucleus $\frac{A_1-1}{Z}X$ and the state of the free, intermediate neutron. Thus $\psi_{\mu1n}(\mathbf{x}_1, \mathbf{x}_{n1}) = V^{-1} e^{i\mathbf{k}_1 \cdot \mathbf{x}_1} e^{i\mathbf{k}_n \cdot \mathbf{x}_{n1}}$ and it has the form in the coordinates $\mathbf{R}_1, \mathbf{r}_{n1}$

$$\psi_{\mu1n}(\mathbf{R}_1, \mathbf{r}_{n1}) = V^{-1} e^{i(\mathbf{k}_1 + \mathbf{k}_n) \cdot \mathbf{R}_1} e^{i(\mathbf{k}_n - \frac{\mathbf{k}_1}{A_1-1}) \cdot \mathbf{r}_{n1}}, \quad (61)$$

where \mathbf{k}_1 and \mathbf{k}_n are the wave vectors of the nucleus $\frac{A_1-1}{Z}X$ and the neutron, respectively.

The intermediate state may have an other form

$$\Psi_\mu(\mathbf{x}_e, \mathbf{x}_1, \mathbf{x}_{n1}, \mathbf{x}_2) = \psi_{fe}(\mathbf{x}_e) \psi_{f1}(\mathbf{x}_1) \psi_{\mu2n}(\mathbf{x}_{n1}, \mathbf{x}_2), \quad (62)$$

where

$$\psi_{\mu2n}(\mathbf{x}_{n1}, \mathbf{x}_2) = \psi_n(\mathbf{x}_{n1}) \psi_{i2}(\mathbf{x}_2) = V^{-1} e^{i\mathbf{k}_n \cdot \mathbf{x}_{n1}} e^{i\mathbf{k}_{i2} \cdot \mathbf{x}_2} \quad (63)$$

which can be written in the coordinates $\mathbf{r}_{n2} = \mathbf{x}_{n1} - \mathbf{R}_2$ and $\mathbf{R}_2 = (A_2\mathbf{x}_2 + \mathbf{x}_{n1}) / (A_2 + 1)$ as

$$\psi_{\mu2n}(\mathbf{R}_2, \mathbf{r}_{n2}) = \frac{1}{V} e^{i(\mathbf{k}_{i2} + \mathbf{k}_n) \cdot \mathbf{R}_2} e^{i(\mathbf{k}_n - \frac{\mathbf{k}_{i2}}{A_2}) \cdot \mathbf{r}_{n2}}, \quad (64)$$

where \mathbf{R}_2 is the center of mass coordinate of the nucleus $\frac{A_2+1}{Z}X$ and \mathbf{r}_{n2} is the relative coordinate of the neutron in it. In these new variables $\mathbf{x}_2 = \mathbf{R}_2 - \mathbf{r}_{n2}/A_2$ and $\mathbf{x}_{n1} - \mathbf{x}_2 = (A_2 + 1)\mathbf{r}_{n2}/A_2$ which is used in the argument of V^{St} (given by (12)) in calculating $V_{f\mu}^{St}$. Evaluating the matrix elements $V_{\mu i}^{Cb}$ and $V_{f\mu}^{St}$ the forms (61) and (64) of ψ_μ are used, respectively, and $\sum_\mu \rightarrow \frac{V}{(2\pi)^3} d^3 k_n$ in (14).

The final state has the form

$$\Psi_f(\mathbf{x}_e, \mathbf{x}_1, \mathbf{x}_{n1}, \mathbf{x}_2) = \psi_{fe}(\mathbf{x}_e) \psi_{f1}(\mathbf{x}_1) \psi_{f2n}(\mathbf{x}_{n1}, \mathbf{x}_2), \quad (65)$$

where $\psi_{f2n}(\mathbf{x}_{n1}, \mathbf{x}_2)$ is given in the variables $\mathbf{R}_2, \mathbf{r}_{n2}$ as

$$\psi_{f2n}(\mathbf{R}_2, \mathbf{r}_{n2}) = V^{-1/2} \exp(i\mathbf{k}_2 \cdot \mathbf{R}_2) \Phi_{f2}(\mathbf{r}_{n2}), \quad (66)$$

and $\Phi_{f2}(\mathbf{r}_{n2})$ is the bound state of the neutron in the nucleus $\frac{A_2+1}{Z}X$.

B. Evaluation of matrix elements $V_{\mu i}^{Cb}$ and $V_{f\mu}^{St}$

The argument of the Coulomb potential V^{Cb} is $\mathbf{x}_e - \mathbf{x}_1$ therefore the integration with respect to the components

of \mathbf{x}_2 may be carried out and $\int |\psi_{i2}(\mathbf{x}_2)|^2 d^3x_2 = 1$. The remainder is

$$V_{\mu i}^{Cb} = \int \psi_{fe}^*(\mathbf{x}_e) \psi_{\mu 1n}^*(\mathbf{x}_1, \mathbf{x}_{n1}) V^{Cb}(\mathbf{x}_e - \mathbf{x}_1) \times \psi_{ie}(\mathbf{x}_e) \psi_{i1n}(\mathbf{x}_1, \mathbf{x}_{n1}) d^3x_e d^3x_1 d^3x_{n1}. \quad (67)$$

Making the $\mathbf{x}_1, \mathbf{x}_{n1} \rightarrow \mathbf{R}_1, \mathbf{r}_{n1}$ change in the variables, substituting the forms (58) and (61) of ψ_{i1n} and $\psi_{\mu 1n}$, and neglecting \mathbf{k}_{i1} , the integrations over the components of \mathbf{x}_e and \mathbf{R}_1 result $V^{-1} (2\pi)^3 \delta(\mathbf{q} + \mathbf{k}_{ie} - \mathbf{k}_{fe})$ and $V^{-3/2} (2\pi)^3 \delta(\mathbf{q} - \mathbf{k}_1 - \mathbf{k}_n)$, respectively and the integration over the components of \mathbf{r}_{n1} produces $F_1(\mathbf{k}_n)$ where

$$F_1(\mathbf{k}_n) = \int \Phi_{i1}(\mathbf{r}_{n1}) e^{-i(\mathbf{k}_n - \frac{\mathbf{k}_1 + \mathbf{q}}{A_1 - 1}) \cdot \mathbf{r}_{n1}} d^3r_{n1}. \quad (68)$$

Using the $\delta(\mathbf{q} + \mathbf{k}_{ie} - \mathbf{k}_{fe})$ in carrying out the integration over the components of \mathbf{q} in $V_{\mu i}^{Cb}$ one gets

$$V_{\mu i}^{Cb} = -\frac{4\pi e^2 Z}{|\mathbf{k}_{fe} - \mathbf{k}_{ie}|^2 + \lambda^2} \tilde{F}_1(\mathbf{k}_n) \frac{(2\pi)^6}{V^{5/2}} \times \times \sqrt{G_S} \delta(\mathbf{k}_{ie} - \mathbf{k}_{fe} - \mathbf{k}_1 - \mathbf{k}_n) \quad (69)$$

and

$$\tilde{F}_1(\mathbf{k}_n) = \int \Phi_{i1}(\mathbf{r}_{n1}) e^{-i(\mathbf{k}_n - \frac{\mathbf{k}_1 + \mathbf{k}_{fe} - \mathbf{k}_{ie}}{A_1 - 1}) \cdot \mathbf{r}_{n1}} d^3r_{n1}. \quad (70)$$

For particles e and 1 (ingoing electron of charge $-e$ and initial nucleus ${}^A_Z X$ of charge Ze) taking part in Coulomb interaction we have used plane waves therefore the matrix element must be corrected with the so called Sommerfeld factor [24] $\sqrt{G_S}$ where

$$G_S = \frac{F_e(E_{ie})}{F_e(E_{f1})}. \quad (71)$$

Now we deal with $V_{f\mu}^{St}$. The strong interaction works between the neutron and the nucleons of the nucleus ${}^A_Z X$ therefore the argument of V^{St} is $\mathbf{x}_{n1} - \mathbf{x}_2$. The integrations with respect to the components of \mathbf{x}_e and \mathbf{x}_1 result $\int |\psi_{ef}(\mathbf{x}_e)|^2 d^3x_e = \int |\psi_{f1}(\mathbf{x}_1)|^2 d^3x_1 = 1$. The remainder is

$$V_{f\mu}^{St} = \int \psi_{f2n}^* V^{St}(\mathbf{x}_{n1} - \mathbf{x}_2) \psi_{\mu 2n} d^3x_2 d^3x_{n1}. \quad (72)$$

Similarly to the above, making the $\mathbf{x}_{n1}, \mathbf{x}_2 \rightarrow \mathbf{R}_2, \mathbf{r}_{n2}$ change in the variables, substituting the forms (64) and (66) of $\psi_{\mu 2n}$ and ψ_{f2n}^* and neglecting \mathbf{k}_{i2} , the integrations over the components of \mathbf{R}_2 result $V^{-3/2} (2\pi)^3 \delta(\mathbf{k}_n - \mathbf{k}_2)$ and the integrations with respect to the components of \mathbf{r}_{n2} produces $F_2(\mathbf{k}_n)$ with

$$F_2(\mathbf{k}_n) = \int \Phi_{f2}^*(\mathbf{r}_{n2}) e^{i\mathbf{k}_n \cdot \mathbf{r}_{n2}} \times \left(-f \frac{\exp(-s \frac{A_2 + 1}{A_2} r_{n2})}{\frac{A_2 + 1}{A_2} r_{n2}} \right) d^3r_{n2}, \quad (73)$$

where $r_{n2} = |\mathbf{r}_{n2}|$. Taking into account that the neutron interacts with each nucleon of the final nucleus of nucleon number A_2

$$V_{f\mu}^{St} = \frac{(2\pi)^3}{V^{3/2}} A_2 F_2(\mathbf{k}_n) \delta(\mathbf{k}_n - \mathbf{k}_2). \quad (74)$$

C. Transition probability per unit time of electron assisted neutron exchange process

Substituting the obtained forms of $V_{\mu i}^{Cb}$ and $V_{f\mu}^{St}$ (formulae (69) and (74)) into (14) and using the correspondence $\sum_{\mu} \rightarrow \frac{V}{(2\pi)^3} d^3k_n$ and the $\delta(\mathbf{k}_n - \mathbf{k}_2)$ in the integration over the components of \mathbf{k}_n one gets

$$T_{fi} = -\frac{4\pi e^2 Z A_2 \tilde{F}_1(\mathbf{k}_2) F_2(\mathbf{k}_2) \sqrt{\frac{F_e(E_{ie})}{F_e(E_{f1})}}}{|\mathbf{k}_{fe} - \mathbf{k}_{ie}|^2 + \lambda^2} \times \frac{(2\pi)^6}{V^3} \frac{\delta(\mathbf{k}_1 + \mathbf{k}_2 + \mathbf{k}_{fe} - \mathbf{k}_{ie})}{(\Delta E_{\mu i})_{\mathbf{k}_n = \mathbf{k}_2}}, \quad (75)$$

where

$$\tilde{F}_1(\mathbf{k}_2) = \int \Phi_{i1}(\mathbf{r}_{n1}) e^{-i(\mathbf{k}_2 - \frac{\mathbf{k}_1 + \mathbf{k}_{fe} - \mathbf{k}_{ie}}{A_1 - 1}) \cdot \mathbf{r}_{n1}} d^3r_{n1} \quad (76)$$

and $F_2(\mathbf{k}_2)$ is determined by (26). Here Φ_{i1} and Φ_{f2} in (26) are the initial and final bound neutron states. Substituting the above into (13), using the identities $[\delta(\mathbf{k}_1 + \mathbf{k}_2 + \mathbf{k}_{fe} - \mathbf{k}_{ie})]^2 = \delta(\mathbf{k}_1 + \mathbf{k}_2 + \mathbf{k}_{fe} - \mathbf{k}_{ie}) \delta(\mathbf{0})$ and $(2\pi)^3 \delta(\mathbf{0}) = V$, the $\sum_f \rightarrow \sum_{m_2} \int [V / (2\pi)^3]^3 d^3k_1 d^3k_2 d^3k_{fe}$ correspondence, averaging over the quantum number m_1 and integrating over the components of \mathbf{k}_{fe} (which gives $\mathbf{k}_{fe} = -\mathbf{k}_1 - \mathbf{k}_2 + \mathbf{k}_{ie}$) one obtains

$$W_{fi} = \int \frac{64\pi^3 \alpha_f^2 \hbar c^2 Z^2 \sum_{l_2 = -m_2}^{l_2 = m_2} |F_2(\mathbf{k}_2)|^2}{v_c V (|\mathbf{k}_1 + \mathbf{k}_2|^2 + \lambda^2)^2 (\Delta E_{\mu i})_{\mathbf{k}_n = \mathbf{k}_2}^2} \times \langle |F_1(\mathbf{k}_2)|^2 \rangle \frac{F_e(E_{ie})}{F_e(E_{f1})} A_2^2 r_{A_2} \delta(E_f - \Delta) d^3k_1 d^3k_2, \quad (77)$$

where A_1, A_2 are the initial atomic masses, l_1, m_1 and l_2, m_2 are the orbit and its projection quantum numbers of the neutron in its initial and final state. For $F_1(\mathbf{k}_2)$, $\langle |F_1(\mathbf{k}_2)|^2 \rangle$ and $F_2(\mathbf{k}_2)$ see (24), (25) and (26). Taking into account the effect of the number of atoms of atomic number A_2 in the solid target the calculation is similar to the calculation of e.g. the coherent neutron scattering [25] and the $|T_{fi}|^2$ must be multiplied by N_L which is the number of atomic sites in the crystal and by r_{A_2} which is the relative natural abundance of atoms ${}^A_Z X$. We have used $N_L / V = 2/v_c$ with v_c the volume of the elementary cell of the fcc lattice in which there are two lattice sites in the cases of Ni and Pd investigated.

D. Approximations, identities and relations in calculation of cross section

Now we deal with the energy denominator ($\Delta E_{\mu i}$) in (77) and (23) [see (15) – (22)]. The shielding parameter λ is determined by the innermost electronic shell of the atom ${}^A_Z X$ and it can be determined as

$$\lambda = \frac{Z}{a_B}, \quad (78)$$

where $a_B = 0.53 \times 10^{-8} \text{ cm}$ is the Bohr-radius. The integrals in (77) and (23) have accountable contributions if

$$|\mathbf{k}_1 + \mathbf{k}_2| \lesssim \lambda \quad (79)$$

and then $E_{fe} \lesssim \hbar^2 \lambda^2 / (2m_e) = \frac{1}{2} \alpha_f^2 m_e c^2 Z^2$ which can be neglected in $\Delta E_{\mu i}$ and in the energy Dirac-delta. Thus

$$\Delta E_{\mu i} = \frac{\hbar^2 \mathbf{k}_1^2}{2m_1} + \frac{\hbar^2 \mathbf{k}_2^2}{2m_n} - \Delta_- + \Delta_n \quad (80)$$

and in the Dirac-delta

$$E_f = \frac{\hbar^2 \mathbf{k}_1^2}{2m_1} + \frac{\hbar^2 \mathbf{k}_2^2}{2m_2}. \quad (81)$$

In this case $\mathbf{k}_1 = -\mathbf{k}_2 + \delta \mathbf{k}$ with $|\delta \mathbf{k}| = \delta k \sim \lambda$. Using

$$k_1 \simeq k_2 \simeq k_0 = \sqrt{2\mu_{12}\Delta}/\hbar \quad (82)$$

(see below) with $\mu_{12}c^2 = A_{12}m_0c^2$, where $A_{12} = (A_1 - 1)(A_2 + 1)/(A_1 + A_2)$ is the reduced nucleon number, one can conclude that the $\mathbf{k}_2 = -\mathbf{k}_1$ relation fails with a very small error in the cases of events which fulfill condition (79) since $k_1/k_0 \simeq 1$, $k_2/k_0 \simeq 1$, $\delta k/k_0 \sim \lambda/k_0$ and $\lambda/k_0 = \alpha_f Z m_e c^2 / \sqrt{2\mu_{12}c^2\Delta} \ll 1$. Consequently, the quantity E_f in the argument of the energy Dirac-delta can be written approximately as

$$E_f = \left(\frac{\hbar^2}{2m_1} + \frac{\hbar^2}{2m_2} \right) \mathbf{k}_2^2 = \frac{\hbar^2 c^2 \mathbf{k}_2^2}{2A_{12}m_0c^2}. \quad (83)$$

Furthermore taking $A_1/(A_1 + 1) \simeq 1$

$$\Delta E_{\mu i} = \frac{\hbar^2 c^2 \mathbf{k}_2^2}{2m_0c^2} - \Delta_- + \Delta_n. \quad (84)$$

We introduce the $\mathbf{Q} = \hbar c \mathbf{k}_2 / \Delta$, $\mathbf{P} = \hbar c (\delta \mathbf{k}) / \Delta$, $\varepsilon_f = E_f / \Delta = [\mathbf{Q}^2 / (2A_{12}m_0c^2)] \Delta$ and $L = \hbar c \lambda / \Delta$ dimensionless quantities. The energy Dirac-delta modifies as $\delta(E_f - \Delta) = \delta[\varepsilon_f(\mathbf{Q}) - 1] / \Delta$. The relation (78) yields $L = \hbar c Z / (a_B \Delta) = Z \alpha_f m_e c^2 / \Delta$ and $Z \alpha_f m_e c^2 / \Delta \lesssim 1$. Now we change $d^3 k_1 d^3 k_2$ to $\left(\frac{\Delta}{\hbar c}\right)^6 d^3 Q d^3 P$ in the integration in (23), use the $\delta[g(Q)] = \delta(Q - Q_0) / g'(Q_0)$ identity, where Q_0 is the root of the equation $g(Q) = 0$ ($k_0 = Q_0 \Delta / (\hbar c)$, see (82)), estimate the integral with respect to the components of \mathbf{P} by

$$\int_0^\infty \frac{4\pi P^2 dP}{(P^2 + L^2)^2} = \frac{\pi^2}{L} \quad (85)$$

and apply $v_c = d^3/4$ (the volume of unit cell of *fcc* lattice for *Ni* and *Pd* of lattice parameter d).

E. $\langle |F_1(\mathbf{k}_0)|^2 \rangle_{Sh}$ and $\sum_{l_2=-m_2}^{l_2=m_2} |F_2(\mathbf{k}_0)|_{Sh}^2$ in single particle shell-model and without LWA

Now we calculate the quantities $\langle |F_1(\mathbf{k}_0)|^2 \rangle_{Sh}$ and $\sum_{l_2=-m_2}^{l_2=m_2} |F_2(\mathbf{k}_0)|_{Sh}^2$ in the single particle shell model with isotropic harmonic oscillator potential and without the long wavelength approximation (see definitions: (24), (25) and (26)). Taking into account the spin-orbit coupling in the level scheme the emerging neutron states are $0l$ and $1l$ shell model states in the cases of *Ni* and *Pd* to be discussed numerically [26]. So the initial and final neutron states (Φ_{i1}, Φ_{f2}) have the form

$$\Phi_{Sh}(\mathbf{r}_{nj}) = \frac{R_{n_j l_j}}{r_{n_j}} Y_{l_j m_j}(\Omega_j) \quad (86)$$

where $n_j = 0, 1$ in the cases of $0l$ and $1l$ investigated, respectively, and

$$R_{0l_j} = b_j^{-1/2} \left(\frac{2}{\Gamma(l_j + 3/2)} \right)^{1/2} \varrho_j^{l_j+1} \exp\left(-\frac{1}{2}\varrho_j^2\right), \quad (87)$$

$$R_{1l_j} = b_j^{-1/2} \left(\frac{2l_j + 3}{\Gamma(l_j + 3/2)} \right)^{1/2} \varrho_j^{l_j+1} \times \left(1 - \frac{2}{2l_j + 3} \varrho_j^2 \right) \exp\left(-\frac{1}{2}\varrho_j^2\right) \quad (88)$$

with $\varrho_j = r_{n_j}/b_j$ where $b_j = \sqrt{\hbar/(m_0\omega_j)}$ [26]. Here ω_j is the angular frequency of the oscillator that is determined by $\hbar\omega_1 = 40A_1^{-1/3} \text{ MeV}$ and $\hbar\omega_2 = 40(A_2 + 1)^{-1/3} \text{ MeV}$ [27]. (The subscript *Sh* refers to the shell model.) With the aid of these wave functions and for $n_1 = 0, 1$

$$\langle |F_1(\mathbf{k}_0)|^2 \rangle_{Sh} = b_1^3 \frac{2^{l_1+2}}{\sqrt{\pi}(2l_1 + 1)!!} 4\pi I_{1,n_1}^2 \quad (89)$$

with

$$I_{1,0} = \int_0^\infty \varrho^{l_1+2} j_{l_1}(k_0 b_1 \frac{A_1}{A_1 - 1} \varrho) e^{-\frac{1}{2}\varrho^2} d\varrho \quad (90)$$

and

$$I_{1,1} = \left(l_1 + \frac{3}{2} \right) \int_0^\infty \varrho^{l_1+2} \left(1 - \frac{2}{2l_1 + 3} \varrho^2 \right) \times j_{l_1}(k_0 b_1 \frac{A_1}{A_1 - 1} \varrho) e^{-\frac{1}{2}\varrho^2} d\varrho. \quad (91)$$

Here $j_{l_1}(x) = \sqrt{\frac{\pi}{2x}} J_{l_1+1/2}(x)$ denotes spherical Bessel function with $J_{l_1+1/2}(x)$ the Bessel function of first kind.

Similarly

$$\sum_{l_2=-m_2}^{l_2=m_2} |F_2(\mathbf{k}_0)|_{Sh}^2 = b_2 f^2 \frac{2^{l_2+2} (2l_2 + 1)}{\sqrt{\pi} (2l_2 + 1)!!} \times \left(\frac{A_2}{A_2 + 1} \right)^2 I_{2,n_2}^2 \quad (92)$$

with

$$I_{2,0} = \int_0^\infty \rho^{l_2+1} j_{l_2}(k_0 b_2 \rho) e^{-\frac{1}{2}\rho^2 - \frac{A_2+1}{A_2} \frac{b_2}{r_0} \rho} d\rho \quad (93)$$

and

$$I_{2,1} = \left(l_2 + \frac{3}{2}\right) \int_0^\infty \rho^{l_2+1} \left(1 - \frac{2}{2l_2+3} \rho^2\right) \times \quad (94) \\ \times j_{l_2}(k_0 b_2 \rho) e^{-\frac{1}{2}\rho^2 - \frac{A_2+1}{A_2} \frac{b_2}{r_0} \rho} d\rho.$$

Substituting the results of (89), (92) and (27) into (29) one gets

$$\eta_{l_1, n_1, l_2, n_2}(A_1, A_2) = \frac{2^{l_1+l_2+4}}{\pi (2l_1+1)!! (2l_2+1)!!} \times \quad (95) \\ \times \frac{b_1^3 b_2}{r_0^4} \left(\frac{A_2}{A_2+1}\right)^2 I_{1, n_1}^2 I_{2, n_2}^2.$$

F. Coulomb factors $F_{2'3}$ and F_{34} in electron assisted heavy charged particle exchange process

If initial particles have negligible initial momentum then, because of momentum conservation, $\mathbf{k}_{2'} = -\mathbf{k}_5$ in the final state. (It was obtained [16] that the process has accountable cross section if the momentum of the final electron can be neglected, i.e. in the $\mathbf{k}_{1'} \simeq 0$ case.) Thus the condition of energy conservation

$$\frac{\hbar^2 \mathbf{k}_{2'}^2}{2m_{2'}} + \frac{\hbar^2 \mathbf{k}_5^2}{2m_5} = \Delta \quad (96)$$

determines $\mathbf{k}_{2'}$ as

$$\hbar^2 \mathbf{k}_{2'}^2 = 2\mu_{2'5} \Delta, \quad (97)$$

where \hbar is the reduced Planck-constant,

$$\mu_{2'5} = a_{2'5} m_0 c^2 \quad (98)$$

is the reduced rest mass of particles 2' and 5 of mass numbers $A_{2'}$ and A_5 [for $a_{2'5}$ see (5)]. If the initial momenta and the momentum of particle 1' are negligible then $\mathbf{k}_3 = -\mathbf{k}_{2'}$, since momentum is preserved in Coulomb scattering. Thus the energy E_3 of particle 3 can be written as

$$E_3 = \frac{\hbar^2 \mathbf{k}_3^2}{2m_3} = \frac{\mu_{2'5}}{m_3} \Delta = \frac{a_{2'5}}{A_3} \Delta. \quad (99)$$

Calculating the Coulomb factor $F_{2'3}$ [see (3)] between particles 2' and 3 the energy determined by (99) is given in their CM coordinate system (since $\mathbf{k}_3 = -\mathbf{k}_{2'}$) thus it can be substituted directly in (4) producing

$$\eta_{2'3} = (Z_2 - z_3) z_3 \alpha_f A_3 \sqrt{\frac{A_{2'} + A_5}{(A_{2'} + A_3) A_5} \frac{m_0 c^2}{2\Delta}}. \quad (100)$$

Since the above analysis is made in order to discuss the phenomenon of nuclear transmutation we take $A_3 \ll A_{2'} \simeq A_5 = A$ ($\gtrsim 100$ in the case of Pd discussed). So $(A_{2'} + A_5) / [(A_{2'} + A_3) A_5] \simeq 2/A$ and $\eta_{2'3}$ reads approximately as

$$\eta_{2'3} = (Z_2 - z_3) z_3 \alpha_f A_3 \sqrt{\frac{m_0 c^2}{A\Delta}}. \quad (101)$$

Calculating the Coulomb factor F_{34} , the energy of particle 3 determined by (99) is now given in the laboratory frame of reference since particle 4 is at rest. In the CM system of particles 3 and 4 the energy $E_3(CM)$ is

$$E_3(CM) = \frac{A_4 a_{2'5} \Delta}{(A_3 + A_4) A_3}. \quad (102)$$

Substituting it into (4)

$$\eta_{34} = (Z_4 + z_3) z_3 \alpha_f A_3 \sqrt{\frac{m_0 c^2}{2a_{2'5} \Delta}}. \quad (103)$$

Applying the same approximation as above in which $2a_{2'5} \simeq A$

$$\eta_{34} = (Z_4 + z_3) z_3 \alpha_f A_3 \sqrt{\frac{m_0 c^2}{A\Delta}}. \quad (104)$$

Furthermore, if $Z_2 \simeq Z_4 = Z \gg z_3$ then

$$\eta_{2'3} = \eta_{34} = Z z_3 \alpha_f A_3 \sqrt{\frac{m_0 c^2}{A\Delta}}, \quad (105)$$

consequently, $F_{2'3} = F_{34}$.

-
- [1] Fleishmann M and Pons S 1989 *J. Electroanal. Chem.* **261** 301-8
 [2] Krivit S B and Marwan J 2009 *J. Environ. Monit.* **11** 1731-46
 [3] Storms E 2010 *Naturwissenschaften* **97** 861-81
 [4] Angulo C *et al* 1999 *Nucl. Phys. A* **656** 3-183

- [5] Descouvemont P, Adahchour A, Angulo C, Coc A and Vangioni-Flam E, 2004 *At. Dat. Nucl. Dat. Tabl.* **88** 203
 [6] Raiola F *et al* 2002 *Eur. Phys. J. A* **13** 377-82
 [7] Raiola F *et al* 2002 *Phys. Lett. B* **547** 193-9
 [8] Bonomo C *et al* 2003 *Nucl. Phys. A* **719** 37c-42c
 [9] Kasagi J *et al* 2002 *J. Phys. Soc. Japan* **71** 2881-5 (2002)

- [10] Czernski K *et al* 2001 *Europhys. Lett.* **54** 449-55
- [11] Czernski K *et al* 2002 *Nucl. Instr. and Meth. B* **193** 183-7
- [12] Huke A, Czernski K and Heide P 2003 *Nucl. Phys. A* **719** 279c-82c
- [13] Huke A *et al* 2008 *Phys. Rev. C* **78** 015803
- [14] Kálmán P and Keszthelyi T 2004 *Phys. Rev. C* **69** 031606(R)
- [15] Kálmán P and Keszthelyi T 2009 *Phys. Rev. C* **79** 031602(R)
- [16] Kálmán P and Keszthelyi T 2013 *arXiv*:1312.5498
- [17] Kálmán P and Keszthelyi T 2013 *arXiv*:1303.1078
- [18] Kálmán P and Keszthelyi T 2012 *arXiv*:1312.5835
- [19] Alder K *et al* 1956 *Rev. Mod. Phys.* **28** 432-542
- [20] Bjorken J D and Drell S D 1964 *Relativistic Quantum Mechanics* (New York: McGraw-Hill)
- [21] Firestone R B and Shirly V S 1996 *Tables of Isotopes* 8th ed (New York: Wiley)
- [22] Rossi A 2009 *Method and Apparatus for Carrying out Nickel and Hydrogen Exothermal Reactions* patent International Publication Number WO 2009/125444 A1 15 October 2009
- [23] Levi G *et al* 2014 <http://www.sifferkoll.se/sifferkoll/wp-content/uploads/>
- [24] Heitler W 1954 *The Quantum Theory of Radiation* 3rd ed (Oxford: Clarendon) chapter V.25 (19)
- [25] Kittel C 1964 *Quantum Theory of Solids* 2nd ed (New York: Wiley) chapter 19
- [26] Pal M K 1983 *Theory of Nuclear Structure* (New York: Scientific and Academic Editions)
- [27] Bohr A and Mottelson B R 1969 *Nuclear Structure* (New York: Benjamin) vol 1